Effect of Variable Viscosity, Arrhenius Activation on Non-Darcy Convective Heat Transfer Flow of SWCNT And MWCNT in a Vertical Channel with Heat Sources

Dr.Y Madhusudhana Reddy
Associate Professor,
Dept of Mathematics,
Sri Venkateswara Degree & PG College,
Anantapur, Andhrapradesh-515001

Article Info
Page Number: 637 – 657
Publication Issue:
Vol 69 No. 1 (2020)

Article History
Article Received: *25 October 2020*
Revised: *30 November 2020*
Accepted: *15 December 2020*

Abstract

In this paper, the combined influence of Arrhenius activation, on non-Darcy hydro magnetic convective heat and mass transfer of a nanofluid in vertical channel with SWCNT and MWCNT. The coupled nonlinear equations governing flow heat transfer have been analyzed by adopting Runge-Kutta fourth order with shooting technique. The effect of variable viscosity, activation energy, heat sources, chemical reaction on the flow characteristic have been studied graphically. The Skin friction, the rate of heat and mass transfer are numerically evaluated for different parametric variations. A rise in velocity and temperature and decay in concentration is noticed with rising values of variable viscosity (B), activation energy (E1) and a depreciation is noticed in them with higher values of temperature different parameter (δ).

Keywords: - Vertical channel, variable viscosity, activation energy, thermal radiation, dissipation, SWCNT, MWCNT.

Activation energy which is an important concenpt related to a chemical kinetics is often studied under physical chemistry. In the year 1889, Swedish scientist, Svante Arrhenius used the term Activation Energy. Present improvements in the computation and understanding of a kinetic method's activation energy are explained. The direct estimation of the energy required to activate for an infinite cyclical timeframe from simulations at a single temperature, in specific, is currently addressed via statistical mechanics' fluctuation theory applied to kinetics.This opens up new options for active processes in situations when a typical Arrhenius analysis is not practicable. The strategies aid in the systematic deconstruction of activation energy into components associated with the system's many interactions and movements. These components can be understood using Tolman's understanding of activation energy. Researchers specifically give insight into how energy might be most efficiently injected in order to speed up a mechanism of specialty, promising significant new structural knowledge for future research. Several authors have been evaluated to effect of Arrhenius activation energy and dual stratifications on the MHD flow of a Maxwell nanofluid with various heating (Sandhya et al. [23], Zeeshan et al. [27], Saida Rashid et al. [22], Gayathri[6], Gireesha et al. [8]). Khan et al [14], Ijaj Khan et al [11], made brief discussion on Activation Energy impact in Nonlinear Radiative Stagnation Point Flow of Cross Nanofluid and also analysed the Arrhenius activation energy impact in binary chemically reactive flow of TiO_2-Cu-H_2O hybrid nanomaterial.

Nanofluids are solid-liquid composite materials consisting of solid nanoparticles or nanofibers, with sizes typically on the order of 1–100 nm, suspended in a liquid. Nanofluids are characterized by an enrichment of a base fluid like water, toluene, ethylene glycol or oil with nanoparticles in variety of types like Metals, Oxides, Carbides, Carbon, Nitrides, etc. Today nanofluid are sought to have wide range of applications in medical application, biomedical industry, detergency, power generation in nuclear reactors and more specifically in any heat removal involved industrial applications. The ongoing research ever since then has extended to utilization of nanofluids in microelectronics, fuel cells, pharmaceutical processes , hybrid-powered engines, engine cooling, vehicle thermal management, domestic refrigerator, chillers, heat exchanger, nuclear reactor coolant, grinding, machining, space technology, Defense and ships, and boiler flue gas temperature reduction [Agarwal et al. [1]]. Indisputably, the nanofluids are more stable and have acceptable viscosity and better wetting, spreading, and dispersion properties on a solid surface [Nguyen et al. [17], Ghadimi[7]].

Thus, nanofluids have an ample collection of potential applications in electronics, pharmaceutical processes, hybrid-powered engines, automotive and nuclear applications where enhanced heat transfer or resourceful heat dissipation is required. In view of these, Kiblinski et al. [15] suggested four possible explanations for the anomalous increase in the thermal conductivity of nanofluids. These are nanoparticles clustering, Brownian motion of the particles, molecular level layering of the liquid/particles interface and ballistic heat transfer in the nanoparticles. Despite a vast amount of literature on the flow of nanofluid model proposed by Buongiorno [3].

A new subcategory of nanomaterials is being created by continued research into nanofluids. Metals, semi-conductors, or composites of nonconductive nanoparticles and carbon nanotubes, including single-wall and multiple-wall carbon nanotubes, were all considered. Ahmed et al. [2] considered carbon nanotubes in an asymmetric channel to examine the flow heat transfer of nanofluids. The bodily characteristics of this fluid in a working base fluid can be varied under the mechanism of an external magnetic field to enhance the usages of the conducting magnetonanoliquid, As such, the usefulness stimulated Ibrahim and Khan [10] to mathematically study the flow of MWCNT-water and SWCNT-water past a stretchable surface. The results revealed that MWCNT-water has a high heat conducting strength than SWCNT-water, as demonstrated in the temperature field. Sheikholeslami [25] numerically investigated the solar system with a turbulator and hybrid nanofluid. Recently Shamshuddin et al[24] were analyzed dynamics of ethylene glycol conveying MWCNTs and ethylene glycol conveying SWCNTs: Significant joule heating and thermal radiation.

CNTs have also received great interest due to significant enhancement of thermal conductivity, unique structure and physical (mechanical and electrical) properties [Ko et al [16]. Ding et al. [5] have prepared a nanofluids with suspension of CNTs in distilled water and measured the thermal conductivity and viscosity of CNTs nanofluids. They have reported the enhancement of thermal conductivity depends on CNTs concentration, and pH level. They also concluded that nanofluids with 0.5 wt.% CNTs, the maximum enhancement is over 350% at Re = 800. And this study noted that the maximum thermal conductivity enhances up to 19.75% for the nanofluid containing 0.45 vol.% MWCNT at 40°C. Youngki Yoon et al[26] studied a vertical partial gate carbon nanotube (CNT) field-effect transistor (FET), which is amenable to the vertical CNT growth process and offers the potential for a parallel CNT array channel, is simulated using a self-consistent atomistic approach. Hazarika and Ahmed [9] analysed the problem of heat/mass transfer in MHD free convective flow of Casson-fluid in a vertical channel embedded with saturated porous medium past through carbon nanotubes in the form of single-wall carbon nanotubes (SWCNTs) and multiple-wall carbon nanotubes (MWCNTs) with engine oil as base fluid. Jingqi Li et al [14] discussed vertically aligned carbon nanotube field-effect transistors.

The constant physical parameters of the fluid, for most realistic fluids, the viscosity shows a rather pronounced variation with temperature. It is known that the fluid viscosity changes with temperature shows a rather pronounced variation with temperature. It is known that the fluid viscosity changes with temperature Das et al.[4]. Thus it is necessary to take into account the variation of viscosity with temperature in order to accurately predict the heat transfer rates. Ali[3] investigated the effect of variable viscosity on mixed convection heat transfer along a moving surface, other effort researchers (Pantokratoras [19,20,21], Kafoussian and Williams[13]) are analyzed the effects of variable viscosity on convective heat transfer along a vertical surface in a saturated porous medium.

In this paper, an attempt has been made to investigate effect of variable viscosity, Arrhinius activation on non-darcy convective heat transfer flow of SWCNT and MWCNT in a vertical channel with heat sources. The nonlinear governing equations have been solved by Runge-Kutta Shooting technique. The effect of variable viscosity, activation energy, heat sources, chemical reaction on the flow characteristic have been studied graphically. The Skin friction, the rate of heat and mass transfer are numerically evaluated for different parametric variations.

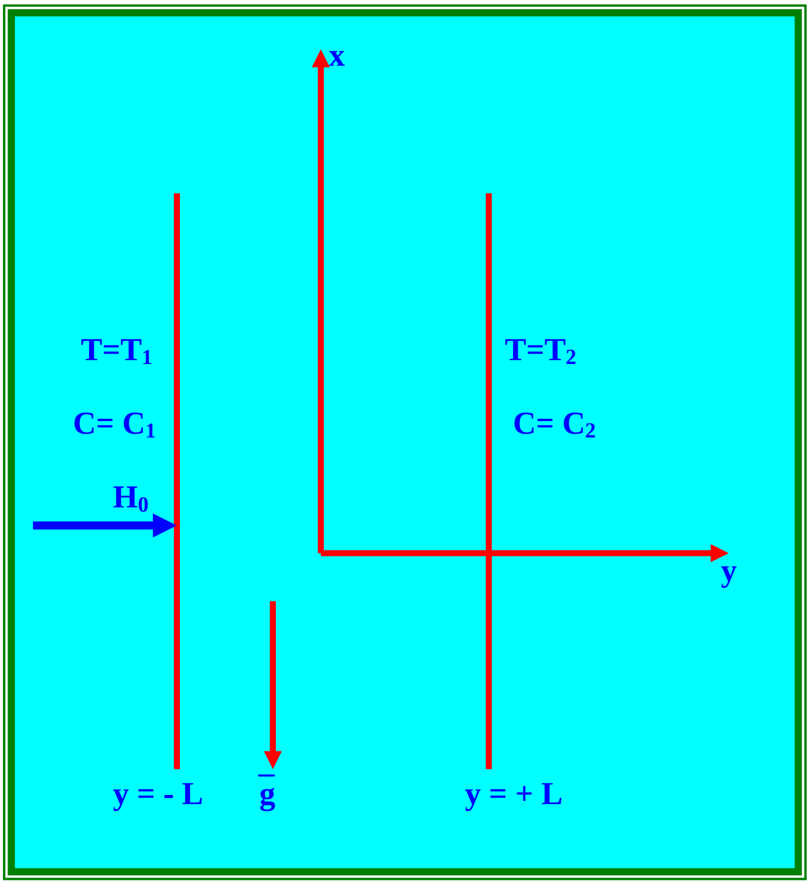

Figure 1 . Schematic diagram of the problem

2. Formulation Of The Problem:

Consider the steady flow of an electrically conducting ,viscous fluid through a porous medium in a vertical channel by flat walls. A uniform magnetic field of strength Ho is applied normal to the walls. Assuming the magnetic Reynolds number to be small we neglect the induced magnetic field in comparison to the applied field. The walls are maintained at constant temperature T_1,T_2 and concentration C_1,C_2 .We consider a rectangular Cartesian coordinate system O(x,y) with x-axis along the walls and y-axis normal to the walls. The walls are taken at $y=\pm L$. The boundary layer equations of flow ,heat and mass transfer under Boussinesq approximation are:

Equation of Continuity

$$\frac{\partial u}{\partial x} + \frac{\partial v}{\partial y} = 0 \tag{2.1}$$

Momentum equation

$$u\frac{\partial u}{\partial x}+v\frac{\partial u}{\partial y}=-\frac{1}{\rho_{nf}}\frac{\partial p}{\partial x}+\frac{1}{\rho_{nf}}\frac{\partial}{\partial y}(\mu_{nf}(T)\frac{\partial u}{\partial y})-\frac{\sigma B(x)^2}{\rho_{nf}}u-\frac{1}{\rho_{nf}}\frac{\mu_f(T)}{k_p}u- \\ -\frac{1}{\rho_{nf}}g(1-C_0)\beta\rho_f\beta g(T-T_0)-(\rho_p-\rho_f)g(C'-C_0)-\frac{1}{\rho_{nf}}\frac{C_b}{\sqrt{k_p}}u^2 \qquad (2.2)$$

$$u\frac{\partial v}{\partial x}+v\frac{\partial v}{\partial y}=-\frac{1}{\rho_{nf}}\frac{\partial p}{\partial y}+\frac{1}{\rho_{nf}}\frac{\partial}{\partial y}(\mu_{nf}(T)\frac{\partial v}{\partial y})-\frac{\sigma_{nf}B(x)^2}{\rho_{nf}}u- \\ -\frac{1}{\rho_{nf}}\frac{\mu_{nf}(T)}{k_p}v-\frac{1}{\rho_{nf}}\frac{C_b}{\sqrt{k_p}}v^2 \qquad (2.3)$$

Energy equation

$$u\frac{\partial T}{\partial x}+v\frac{\partial T}{\partial y}=(\frac{k_{nf}}{(\rho C_p)_{nf}})(\frac{\partial^2 T}{\partial x^2}+\frac{\partial^2 T}{\partial y^2})+\frac{Q_H}{(\rho C_p)_{nf}}(T-T_0)+\frac{\alpha_f\mu_f(T)}{(\rho C_p)_{nf}}(\frac{\partial u}{\partial y})^2+ \\ +\frac{\sigma B(x)^2}{(\rho C_p)_{nf}}(u^2)+\frac{Q_1'}{(\rho C_p)_{nf}}(C-C_0) \qquad (2.4)$$

Diffusion equation

$$u\frac{\partial C}{\partial x}+v\frac{\partial}{\partial y}=D_B\frac{\partial^2 C}{\partial y^2}-k_c(C-C_0)(\frac{T}{T_0})^n Exp(-\frac{E_n}{kT}) \qquad (2.5)$$

The boundary conditions relevant to the problem are

$$u=U_w(x), v=0, T=T_1, C'=C_1 \quad on\ y=-L \\ u=0, v=0, T=T_2\ C'=C_2 \quad on\ y=+L \qquad (2.6)$$

The effective density of the nanofluid is given by

$$\rho_{nf}=(1-\varphi)\rho_f+\varphi\rho_s \qquad (2.7)$$

Where ϕ is the solid volume fraction of nanoparticles. Thermal diffusivity of the nanofluid is

$$\alpha_{nf}=\frac{k_{nf}}{(\rho C_p)_{nf}} \qquad (2.8)$$

Where the heat capacitance C_p of the nanofluid is obtained as

$$(\rho C_p)_{nf}=(1-\varphi)(\rho C_p)_f+\varphi(\rho C_p)_s \qquad (2.9)$$

And the thermal conductivity of the nanofluid k_{nf} for spherical nanoparticles can be written as

$$\frac{k_{nf}}{k_f}=\frac{(k_s+2k_f)-2\phi(k_f-k_s)}{(k_s+2k_f)+\phi(k_f-k_s)} \qquad (2.10)$$

The thermal expansion coefficient of nanofluid can determine by

$$(\rho\beta)_{nf}=(1-\varphi)(\rho\beta)_f+\varphi(\rho\beta)_s \qquad (2.11)$$

Also the effective dynamic viscosity of the nanofluid given by

$$\mu_{nf}=\frac{\mu_f}{(1-\varphi)^{2.5}},\quad \sigma_{nf}=\sigma_f(1+\frac{3(\sigma-1)\phi}{\sigma+2-(\sigma-1)\phi}),\sigma=\frac{\sigma_s}{\sigma_f} \qquad (2.12)$$

Where the subscripts nf, f and s represent the thermo physical properties of the nanofluid, base fluid and the nanosolid particles respectively and ϕ is the solid volume fraction of the nanoparticles. The thermo physical properties of the nanofluid are given in Table 1.

The thermo physical properties of the nanofluids are given in Table 1 (See ***Oztop and Abu-Nada*** [18]).

Table – 1

Physical properties	Fluid phase (Water)	**Swcnt's**	**Mwcnt's**
C_p(j/kg K)	4179	**425**	**796**
ρ(kg m^3)	997.1	**2600**	**1600**
k(W/m K)	0.613	**6600**	**3000**
βx10^{-5} 1/k)	21	2.0	**2.0**
σ	**0.05**	**10^6**	**10^7**

We now define the following non-dimensional variables

The dynamic viscosity of the nanofluids is assumed to be temperature dependent as follows:

$$\mu_{nf}(T) - \mu_f Exp(-m(T - T_o)) \tag{2.13}$$

where μ_f is the nanofluid viscosity at the ambient temperature To, m is the viscosity variation parameter which depends on the particular fluid.

Eliminating pressure p between equations(2.2)&(2.3) and introducing similarity variables as

$$\eta = (\frac{L}{\mu_0})^{0.5}, u = Lxf', v = -\sqrt{L\mu_0}\, f(\eta), \theta = \frac{T - T_2}{T_1 - T_2}, C = \frac{C' - C_2}{C_1 - C_2}, p' = \frac{pL^2}{\mu_o^2} \tag{2.14}$$

the equations (2-4) reduce to

$$\left.\begin{aligned} &\frac{d^4 f}{d\eta^4} - B(\frac{d^2 f}{d\eta^2}\frac{d\theta}{d\eta} + \frac{df}{d\eta}\frac{d^2\theta}{d\eta^2} + \frac{d\theta}{d\eta}\frac{d^3 f}{d\eta^3}) + B(\frac{d\theta}{d\eta})^2 - K\frac{d\theta}{d\eta}(\frac{df}{d\eta} - f) + K(\frac{df}{d\eta} - B\frac{d\theta}{d\eta}) + \\ &+ e^{B\theta}(2 f_s(\frac{df}{d\eta}\frac{d^2 f}{d\eta^2} - f\frac{df}{d\eta})M^2 f' + Gr(\theta - N_r C)) + f\frac{d^3 f}{d\eta^3} - \frac{df}{d\eta}\frac{d^2 f}{d\eta^2} = \\ &-(\frac{df}{d\eta})^2 - M^2\frac{d^2 f}{d\eta^2}) = 0 \end{aligned}\right| \tag{2.15}$$

$$(A_5 + \frac{4Rd}{3})\frac{d^2\theta}{d\eta^2} + (P_r) f\frac{d\theta}{d\eta} + Q\theta + Ec(e^{-B\theta})(\frac{d^2 f}{d\eta^2})^2 + EcM^2(\frac{df}{d\eta})^2 + Q_1 C \tag{2.16}$$

$$\frac{d^2 C}{d\eta^2} + (Sc) f\frac{dC}{d\eta} - \gamma\, Sc(1 + n\delta\theta)Exp(-\frac{E_1}{1 + \delta\theta}) \tag{2.17}$$

The corresponding boundary conditions are

$$\begin{aligned} &f'(-1) = 1, f(-1) = 0, \theta(-1) = 1, C(-1) = 1 \\ &f'(+1) = 0, f(+1) = 0, \theta(+1) = 0, C(+1) = 0 \end{aligned} \tag{2.18}$$

$$A_1 = \frac{1}{(1-\varphi)^{2.5}}\ ,\ A_2 = (1-\varphi) + \varphi(\frac{\rho_s}{\rho_f}),\ A_3 = 1 - \varphi + \varphi\frac{(\rho C_p)_s}{(\rho C_p)_f}, A_4 = 1 - \varphi + \varphi(\frac{(\rho\beta)_s}{(\rho\beta)_f},$$

$$A_5 = \frac{k_{nf}}{k_f}\quad A_6 = (1 + \frac{3(\sigma - 1)}{\sigma + 2 - (\sigma - 1)\phi}), \sigma_{nf} = \sigma_f A_6, \sigma = \frac{\sigma_s}{\sigma_f}$$

where

$$Gr = \frac{\beta_T g(T_1 - T_2)L^3}{\mu_o^2}, M = \frac{\sigma B_o^2 L^2}{\mu_o}, K = \frac{L^2}{k_p}, B = m(T_1 - T_2),$$

$$Q = \frac{Q_H L^2}{Cp}, \theta_w = \frac{T_1}{T_o}, \delta = \theta_w - 1, E_1 = \frac{E_n}{k_f T_0}, Rd = \frac{4\sigma^\bullet T_o^3}{\beta_R k_f}, Ec = \frac{\mu_0}{k_f L^2(T_1 - T_2)}.$$

$$Sc = \frac{\nu}{D_B}, Q_1 = \frac{Q_1' L^2(C_1 - C_2)}{(\rho C_p)_f(T_1 - T_2)}\ fs = \frac{C_b\mu_o L}{\sqrt{k_p}}, B(x) = \frac{B_0}{\sqrt{x}}, U_w(x) = Lx$$

are the Grashof number, magnetic parameter, Darcy parameter, viscosity parameter, heat source parameter, temperature difference parameter, activation energy parameter, radiation parameter,Eckert number, Schmidt number, radiation absorption parameter, Forchheimer parameter.

3.Numerical Analysis:

The coupled non-linear ODEs(2.15)-(2.16) along with the corresponding Bcs(2.18) are solved by employing the RKF algorithm with Mathematica programming.The numerical solutions are carried out by choosing the step size Δη=0.001.

(i) The coupled non-linear system of equations was transformed into a set of first order Des.

$$f = f_1, f' = f_2, f'' = f_3, f''' = f_4, \theta = f_5, \theta' = f_6, C = f_{7,}, C' = f_8$$

(ii) The system of first order Des are

$$f^{iv} = (Bf_3 f_6 + f_2 f_6 + f_6 f_4) - Bf_6^2 + Kf_6(f_2 - f_1) - K(f_2 - Bf_6) -$$
$$- e^{Bf_5}(2 f_s(f_2 f_3 - f_1 f_2 M^2 f_2 + M^2 f_3 - Gr(f_5) f_1 f_4 + f_2 f_3$$
$$\theta'' = -(\mathrm{Prf_1 f_6} + Ec(e^{-Bf_5} f_3^2 + M^2 f_2^2) + Qf_5 + Q_1 f_7)$$
$$C'' = -Scf_1 f_8 + \gamma Sc(1 + n\delta f_5 e^{-E1/(1+\delta f_5)}$$

The boundary conditions are

$$f_1(\pm 1) = 0,\ f_2(-1) = 1,\ f_2(+1) = 0,\ f_5(-1) = 1,$$
$$f_5(+1) = 0,\ f_6(-1) = 1,\ f_6(+1) = 0$$

(iii) Suittable guess values are chosen for unknown required Bcs.

(iv) RKF technique with shooting method is utilized for step by step integration with the assistance of Mathematica software.

4.Skin Friction. Nusselt And Sherwood Number:

The quantities of physical interest in this analysis are the skin friction, coefficient Cf, local Nusselt number(Nu),local Sherwood number(Sh) which are defined as

$$C_f = \frac{2\tau_w}{\rho u_w^2}, Nu = \frac{xq_w}{\alpha_f (T_1 - T_o)}, Sh = \frac{xm_w}{D_B(C_1 - C_o)} \tag{4.1}$$

where

$$\tau_w = \mu(\frac{\partial u}{\partial y})_{\eta=\pm 1}, q_w = k_{nf}(\frac{\partial T}{\partial y})_{\eta=\pm 1}, m_w = D_B(\frac{\partial C'}{\partial y})_{\eta=\pm 1} \tag{4.2}$$

Substituting equation(4.2) into equation (4.1),we get

$$Cf = (e^{-B\theta}\frac{\partial u}{\partial y})_{\eta=\pm 1}, Nu = -(\frac{\partial \theta}{\partial y})_{\eta=\pm 1}, Sh = -(\frac{\partial C}{\partial y})_{\eta=\pm 1} \tag{4.3}$$

5. Results And Discussion:

In this analysis we investigate the effect of variable viscosity and Arrhenius activation energy on convective heat and mass transfer flow of Swcnt and Mwcnt-water nanofluids in a vertical channel bounded by flat walls which are maintained at uniform temperature and concentration in the presence of heat generating sources.

Figs.2a-2c exhibit the effect of Grashof number(G) on the velocity, temperature and concentration From the profiles we find that the velocity, temperature experience an enhancement while the concentration depreciates in the flow region with increasing values of G. This shows that an increase in G grows the thickness of the momentum, thermal boundary layers and decays solutal layer. We also find that the nanofluid velocity,temperature in the case of Swcnt – water nanofluid is relatively lesser than that of Mwcnt-water nanofluid. This phenomenon has good agreement with the physical realities,while nanoconcentration in Swcnt-water nanofluid is higher than the Mwcnt-water nanofluid..

The effect of magnetic parameter(M) on the flow variables is shown in figs.3a-3c.Fig.3a exhibits the decreasing nature of the velocity profiles for growing strength of magnetic force. Physically ,a retarding force or drag force (Lorentz force) is generated due to the presence of a magnetic force. Upsurge of magnetic force intensifies the Lorentz force and hence the fluid motion in the flow region decreases .In addition ,due to presence of mixed convection ,the fluid reaches the free stream boundary faster. On the other hand the heat measure and the mass of the fluid as depicted in figures 3b and 3c.Hence ,by controlling the magnetic force, the required cooling can be achieved ,which is useful in many engineering applications. For higher values of M we notice a depreciation in temperature and acceleration in concentration in the flow region. Thus higher the magnetic parameter smaller the thickness of the momentum ,thermal ,larger the solutal boundary layers.Also we find that the nanofluid velocity,temperature in the case of Swcnt – water nanofluid is relatively lesser than that of Mwcnt-water nanofluid,while nanoconcentration in Swcnt-water is lager than that in Mwcnt-water nanofluid. This phenomenon has good agreement with the physical realities.The

The effect of porous medium on flow variables can be seen from figs.4a-4c(K). From the profiles we noticed that lesser the porous permeability smaller the velocity, temperature and larger the nanoconcentration in the flow region.The nanofluid velocity,temperature in the case of Swcnt – water nanofluid is relatively lesser than that of Mwcnt-water nanofluid,while nanoconcentration in Swcnt-water is lager than that in Mwcnt-water nanofluid

In the presence of heat generating heat source (Q>0,the velocity,temperature Enhance,nanoconcentration depreciates due to the generation of thermal energy in the flow region(fig.5a-5c).In all the cases the values in Swcnt-water nanofluid are relatively smaller than those in Mwcnt-water nanofluid.

The effect of thermal radiation(Rd) /viscosity variation(B) lead to a to a rise in velocity and decay in concentration,while the temperature reduces with Rd and enhances with increase in viscosity parameter (B) ((figs.6a-6c&9a-9c). This is because an increase in Rd has a tendency to enhance the conduction effects and to increase velocity at each point in the flow region.Threfore higher values of radiation parameter implies higher surface heat flux.In all the cases values of velocity in Swcnt-water are relatively smaller than those in Mwcnt-water nanofluid, while nanoconcentration in Swcnt-water are higher than those in Mwcnt-water nanofluid.

Figs.7a-7c represent the effect of dissipation on the flow variables..From the profiles we find that higher the dissipative energy(Ec) smaller the velocity and nanoconcentration ,larger the temperature.This implies an increase in Ec leads to a decay in momentum , solutal layer thickness while the thermal boundary layer thickness grows with higher values of Ec.The values of velocity and temperature in Swcnt-water nanofluid are relatively smaller than those in Mwcnt-water nanofluid while reverse is true in nanoconcentration.

Figs.8a-8c demonstrate the effect of nanoparticle volume fraction(ϕ)on flow variables.An increase in ϕ leads to a depreciation in velocity, temperature and rise in nanoconcentration in the flow region.The velocity,temperature values in Swcnt-water are smaller than those in Mwcnt-water naofluid while reverse behaviour is true in nanoconcentration.

Figs.10a-10c&11a-11c exhibit the effect of activation energy parameter(E1) and temperature relative parameter(δ).From the profiles we find that the velocity,temperature and nanoparticle concentration dilute with rising values of δ and upsurges with increase in E1.This is due to the fact that an increase in temperature relative parameter(δ) leads to thinning of the thickness of the boundary layers while they become thicker in the flow region.In the case of variation with respect to E1 and δ the values of flow variables are relatively smaller than those in Mwcnt-water nanofluid.

Figs.12a-12c demonstrate the effect of index number (n) on flow variables. From the profiles we find that the velocity,temperature and nanoconcentration upsurge with rising values of index parameter in the flow region.This is due to the fact that increase in index number(n) leads to a decay in thickness of the momentum,thermal and solutal boundary layers.

It is observed from the profiles that the velocity,temperature decay while nanoparticle concentration grows with a rise in Schmidt number(Sc).In fact,Schmidt number expresses the relative contribution of molecular diffusion rate to species diffusion rate in the flow region.. Therefore, a gradual increase in Sc corresponds to a thicker solutal boundary layer, as in evident from fig.13c.In all the cases the values of flow variables in Swcnt-water nanofluid are relatively smaller than those in Mwcnt-water nanofluid(figs.13a-13c).

The effect of chemical reaction on flow variables can be seen from figs.14a-14c.The velocity, temperature and nanopaticle concentration depreciate in the degenerating chemical reaction case.This may be attributed to the fact that an increase in $\gamma>0$ leads to thinning of momentum,thermal and solual boundary layers.In all the cases the values of velocity and temperature are relatively smaller than those in Mwcnt-water nanofluid while reverse is true in nanoconcentration.

An increase in radiation absorption(Q1) leads to a rise in velocity,temperature and decay in actual nanoparticle concentration in the flow region.Consequently,the the thickness of the momentum,thermal boundary layers become thicker,while the solutal layer becomes thinner with higher values of Q1(figs.15a-15c).In all the cases the values of the flow variable in Swcnt-water are relatively smaller than those in Mwcnt-water nanofluid.

An increase in Forchheimer parameter(fs) reduces the velocity,nanoconcentration while temperature upsurges in the flow region.This implies that the increase in inertia and boundary effects results in a thinning of the momentum,solutal boundary layers while thermal boundary layer thickness becomes thicker(figs.16a-16c).

From figs.17a-17c we notice depreciation in velocity , temperature and nanoparticle concentration with rise in Prandtl number.Physically, thermal diffusivity decreases with increasing values of Pr. This indicates that thickness of momentum , thermal and solutal boundary layers become thinner in the flow region.In all the cases the values of the flow variables in Swcnt-water are smaller than those in Mwcnt-water nanofluid.

The skin friction factor(Cf),Nusselt (Nu)and Sherwood number (Sh)at the walls $\eta = \pm 1$ are exhibited in table.2.From the tabular values we observe that Cf enhances at $\eta = \pm 1$ in both Swcnt and Mwcnt nanofluids.The rate of heat transfer reduces with G at $\eta = -1$,for both Swcnt and Mwcnt while at $\eta = +1$,Nu grows with G in both Swcnt and Mwcnt.The rate of mass transfer exhibits an increasing tendency at $\eta = -1$,while at $\eta = +1$,it decays with increasing values of G for both Swcnt and Mwcnt.

With reference to magnetic parameter(M)and prous parameter(K),we notice a decay in Cf at $\eta = \pm 1$ with M/K for both Swcnt and Mwcnt.Nu accelerates with M/K at $\eta = -1$, for Swcnt and Mwcnt.At $\eta = +1$,Nu reduces for Swcnt and enhances for Mwcnt.Sh reduces with M for Swcnt and enhances for Mwcnt at ,while at $\eta = +1$,Sh augments for both Swcnt and Mwcnt.Sh reduces at $\eta = -1$ and enhances at $\eta = +1$ with increasing values of K for both Swcnt and Mwcnt .

Higher the radiative heat flux(Rd),larger Cf,Nu and Sh at $\eta = -1$ for both Swcnt and Mwcnt while at $\eta = +1$,Cf ,Nu enhance,Sh reduces for Swcnt and for Mwcnt,Cf,Sh decay,Nu grows with Rd.

For higher values of viscosity parameter(B),Cf,Sh enhance,Nu reduces at $\eta = -1$ for both Swcnt and Mwcnt. At $\eta = +1$,Cf,Nu enhance,Sh reduces with B for both Swcnt and Mwcnt.

Higher the strength of the heat generating source (Q>0) larger Cf,Sh and smallerNu at $\eta = -1$.At $\eta = +1$,Cf,Nu enhance,Sh reduces for Swcnt while foe Mwcnt,Cf reduces,Nu and Sh enhances with Q.

Increase in activation energy (E1) lenhances Cf, Nu and reduces Sh for vSwcnt and for Mwcnt ,Cf,Sh enhance,Nu reduces.At $\eta = +1$, Cf, Nu and Sh frow for Swcnt while for Mwcnt, Cf, Nu frow, Sh decays with increasing values of E1. In addition, AE (E1) plays an important role in increasing the local heat transfer coefficient.Generally,AE is the minimum amount of energy that is required for a chemical reaction to stimulates atoms or molecules in the reaction.There should a considerable number of atoms whose AE is less than or equal to translational energy in a chemical reaction,hence in many engineering applications,AE may be considered as a better coolant.

For higher values of temperaturte differebce paraneter(δ) we notice a depreciation in Cf,Sh,enhancement in Nu for Swcnt and Mwcnt .At $\eta = +1$,Cf reduces,Nu and Sh enhance with δ for both types of Swcnt and Mwcnt.

Increase in index parameter(n) leads to a fall in Cf,=,rise in Nu,Sh for Swcnt abnd for Mwcnt,Cf,Sf enhances,Nu reduces with n.At $\eta = +1$,Cf,Sh decay,Nu grows for vSwcnt and for Mwcnt ,CfNu grow,Sh decays with n.

An increase in nanoparticle volume fraction(ϕ)reduces Cf,enhances Nu and Sh for Swcnt and for Mwcnt,Cf,Sh grow,Nu decays at η=-1.At η=+1,Cf,Nu reduce,Sh enhances in both Swcnt and Mwcnt nanofluids.

Lesser the molecular diffusivity smaller Cf,Nu and Sh for Swcnt and for Mwcnt,Cf enhances,Nu,Sh reduce at $\eta = -1$.At $\eta = +1$,Cf,Sh reduce,Sh enhances for Swcnt and for Mwcnt,Cf,Nu enhance,Sh reduces with Sc.

The skin friction(Cf) reduces,Nu and Sh enhance in Swcnt nanofluid an for Mwcnt,Cf,Nu and Sh augument at $\eta = -1$in degenerating chemical reaction case (γ>0).At $\eta = +1$,Cf,Nu,Sh reduce for Swcnt and for Mwcnt,Cf enhances,Nu and Sh reduce with γ>0.

An increase in radiation absorption parameter(Q1) leads to a rise in Cf,Sh and fall in Nu for Swcnt and for Mwcnt,Cf,Nu reduces,Sh enhances at $\eta = -1$.At $\eta = +1$,Cf,Nu enhance,Sh reduces at $\eta = -1$with Q1 for both Swcnt and Mwcnt nanofluids.At $\eta = +1$,Cf,Nu enhance,mSh reduces with f sibn both Swcnt and Mwcnt nanofluids.

Increase in temperature ratio(A) leads to rise in Cf,Sh ,fall in Nu for both Swcnt and Mwcnt at $\eta = -1$ .At $\eta = +1$,Cf,Nu enhance,Sh reduces with increasing values of A for both Swcnt and Mwcnt nanofluids.

Lesser the thermal diffusivity smaller Cf,Sh and larger Nu forv Swcnt and for Mwcnt,Cf,Sh enhance,Nu reduces at $\eta = -1$.At $\eta = +1$,Cf,Nu recuce,Sh enhances for Swcnt and for Mwcnt,Cf,Nu and Sh enhance with Pr.

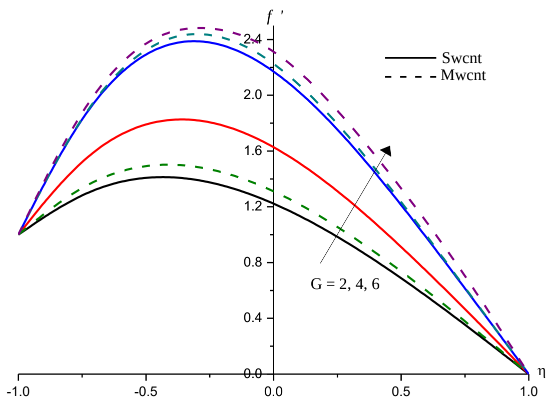

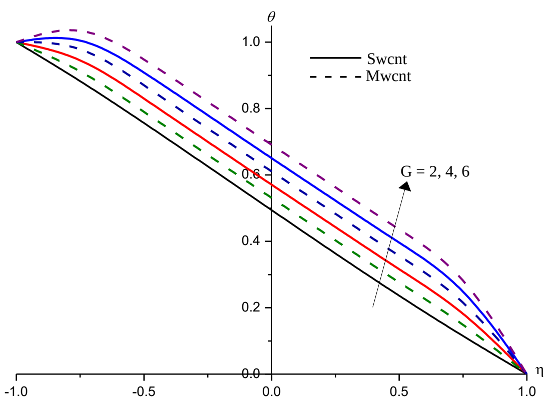

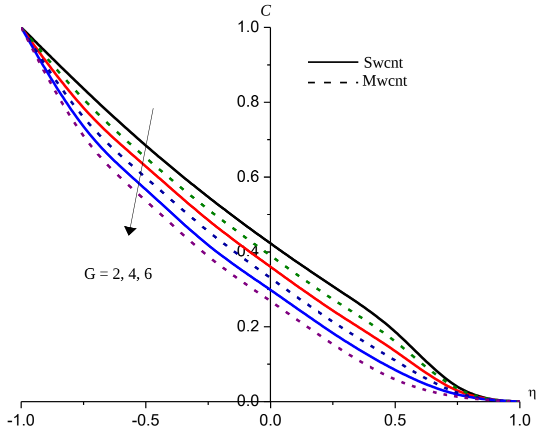

Fig.2 : Variation of [a] Velocity(f'), [b] Temperature(θ), [c] Concentration(C) with G (Swcnt & Mwcnt)
M=0.5, K=0.2, Q=0.5, Rd=0.5, Ec=0.1, ϕ=0.05, B=0.5, E1=0.1, δ=0.2, *n*=1, Sc=0.24, γ=0.5, Q1=0.5, fs=0.1, Pr=0.71

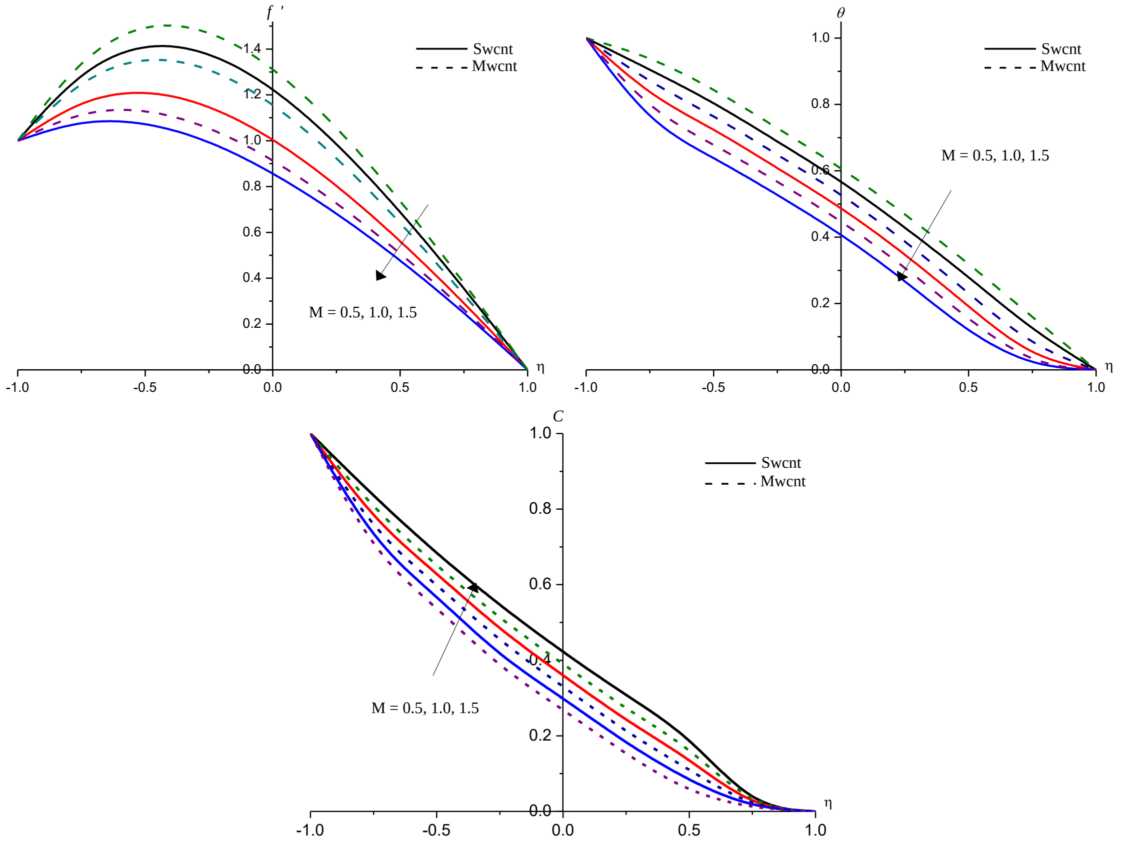

Fig.3 : Variation of [a] Velocity(f'), [b] Temperature(θ), [c] Concentration(C) with M (Swcnt & Mwcnt)
G=2, K=0.2, Q=0.5, Rd=0.5, Ec=0.1, ϕ=0.05, B=0.5, E1=0.1, δ=0.2, *n*=1, Sc=0.24, γ=0.5, Q1=0.5, fs=0.1, Pr=0.71

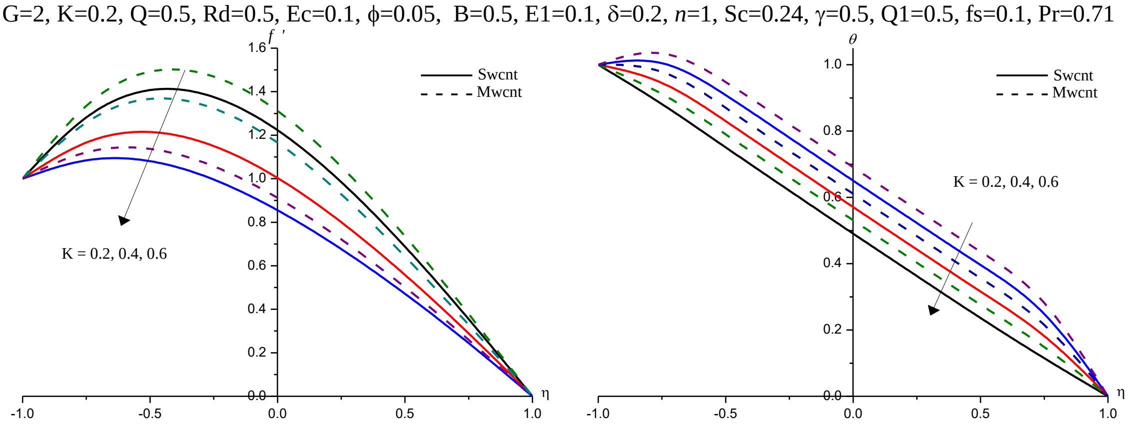

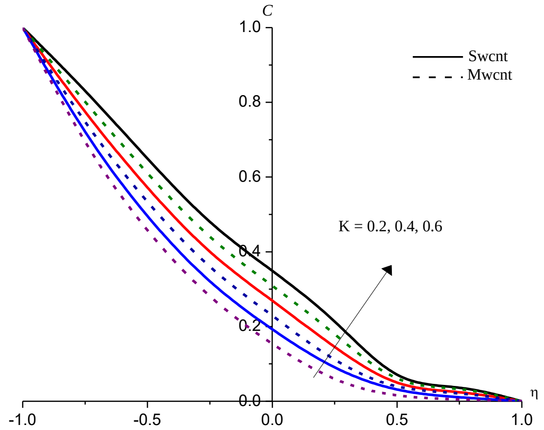

Fig.4 : Variation of [a] Velocity(f'), [b] Temperature(θ), [c] Concentration(C) with K (Swcnt & Mwcnt)
G=2, M=0.5, Q=0.5, Rd=0.5, Ec=0.1, ϕ=0.05, B=0.5, E1=0.1, δ=0.2, *n*=1, Sc=0.24, γ=0.5, Q1=0.5, fs=0.1, Pr=0.71

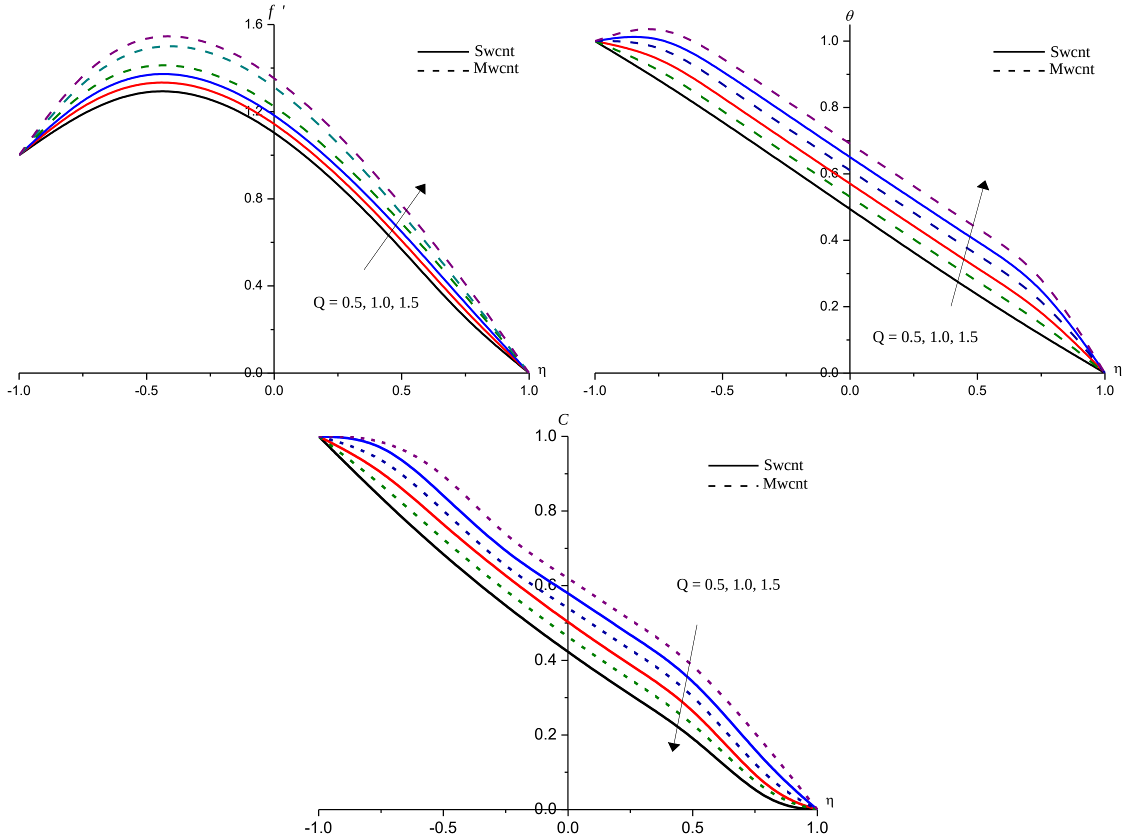

Fig.5 : Variation of [a] Velocity(f'), [b] Temperature(θ), [c] Concentration(C) with Q (Swcnt & Mwcnt)
G=2, M=0.5, K=0.2, Rd=0.5, Ec=0.1, ϕ=0.05, B=0.5, E1=0.1, δ=0.2, *n*=1, Sc=0.24, γ=0.5, Q1=0.5, fs=0.1, Pr=0.71

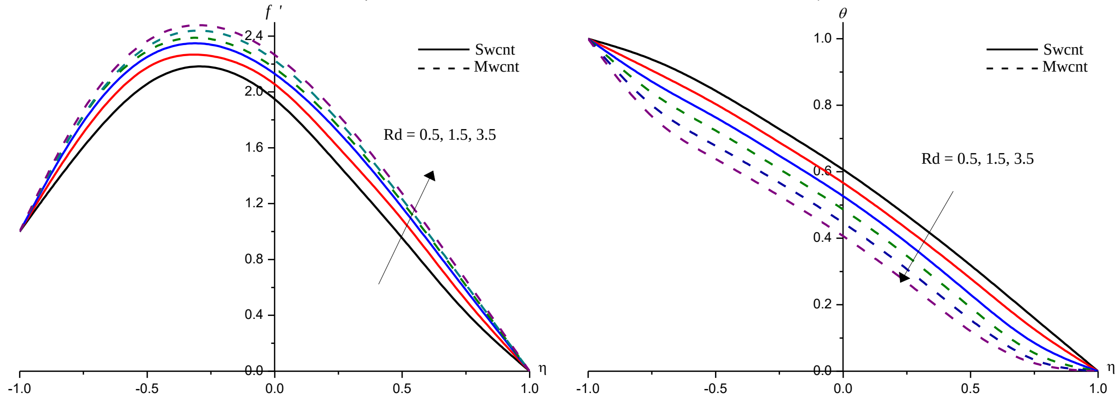

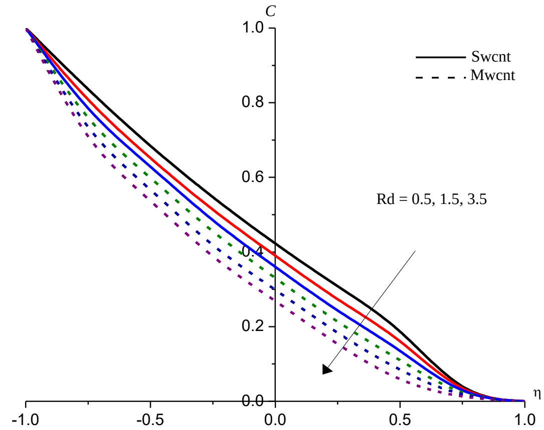

Fig.6 : Variation of [a] Velocity(f'), [b] Temperature(θ), [c] Concentration(C) with Rd (Swcnt & Mwcnt)

G=2, M=0.5, K=0.2, Q=0.5, Ec=0.1, ϕ=0.05, B=0.5, E1=0.1, δ=0.2, *n*=1, Sc=0.24, γ=0.5, Q1=0.5, fs=0.1, Pr=0.71

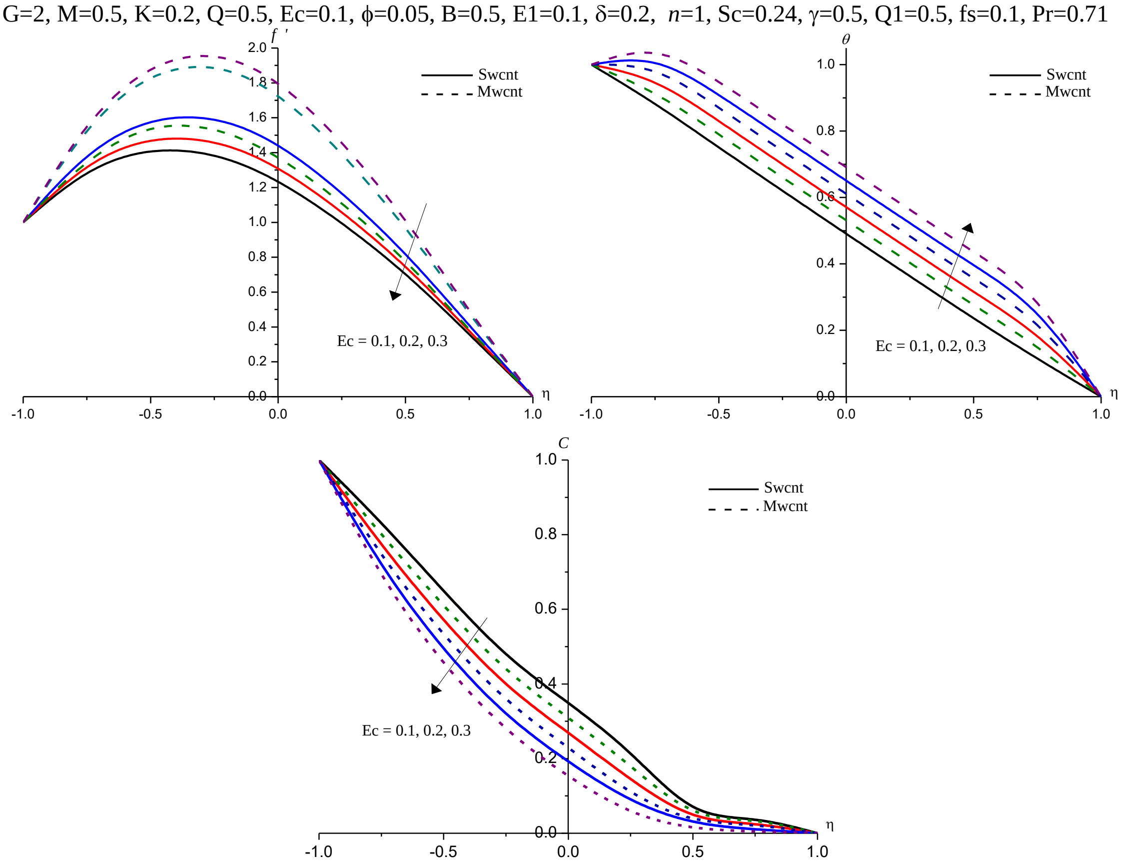

Fig.7 : Variation of [a] Velocity(f'), [b] Temperature(θ), [c] Concentration(C) with Ec (Swcnt & Mwcnt)

G=2, M=0.5, K=0.2, Q=0.5, Rd=0.5, ϕ=0.05, B=0.5, E1=0.1, δ=0.2, *n*=1, Sc=0.24, γ=0.5, Q1=0.5, fs=0.1, Pr=0.71

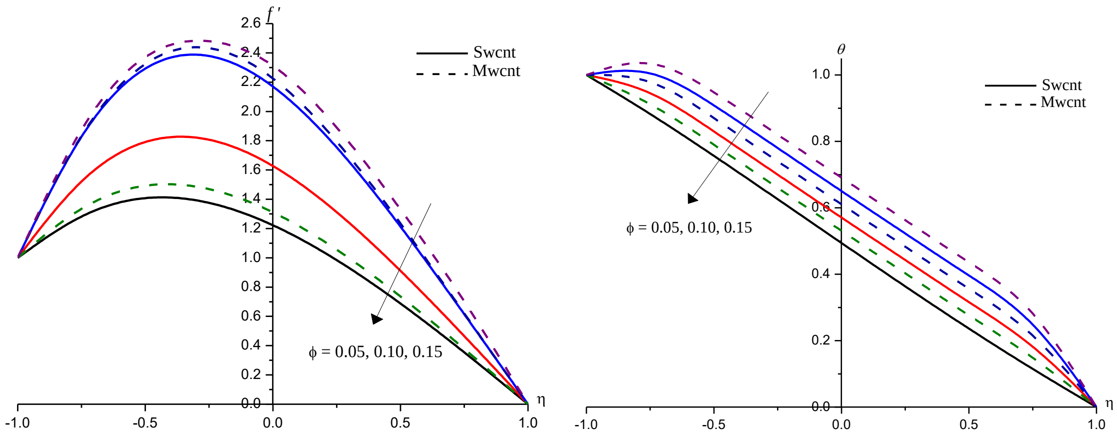

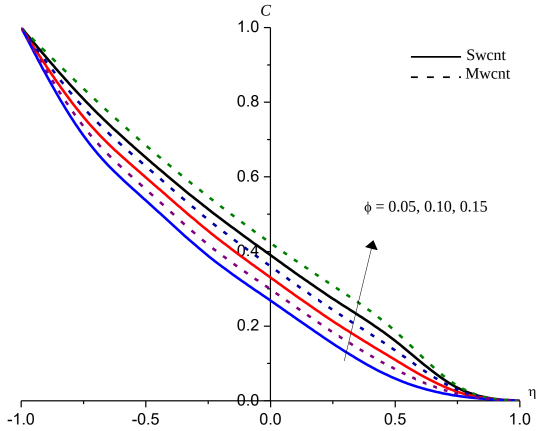

Fig.8 : Variation of [a] Velocity(f'), [b] Temperature(θ), [c] Concentration(C) with ϕ (Swcnt & Mwcnt)
G=2, M=0.5, K=0.2, Q=0.5, Rd=0.5, Ec=0.1, B=0.5, E1=0.1, δ=0.2, n=1, Sc=0.24, γ=0.5, Q1=0.5, fs=0.1, Pr=0.71

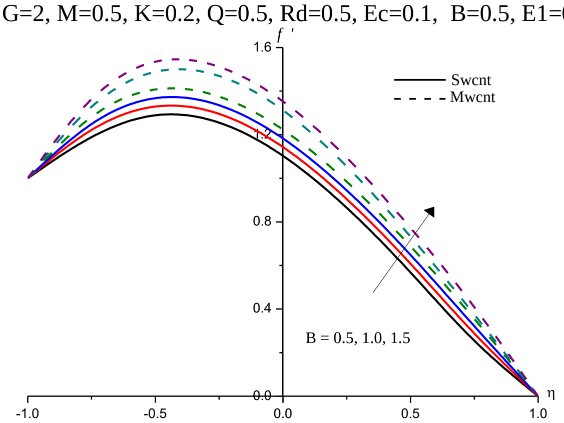

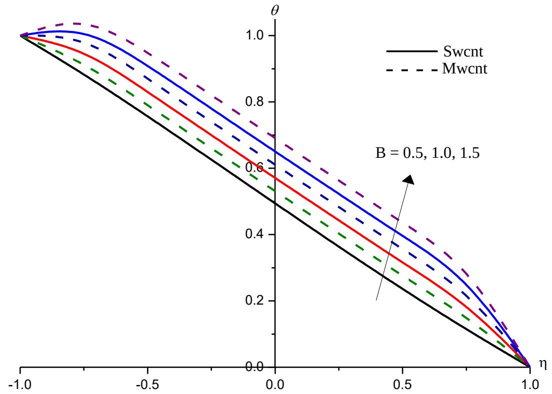

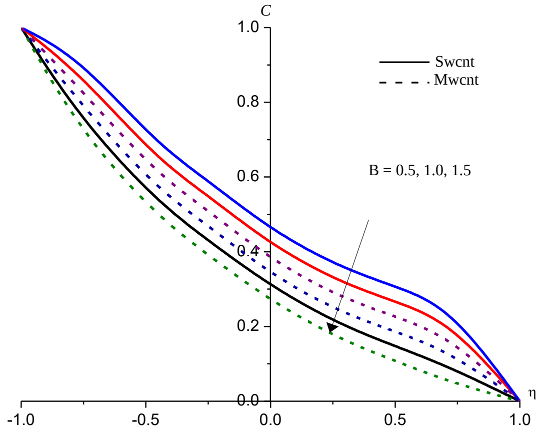

Fig.9 : Variation of [a] Velocity(f'), [b] Temperature(θ), [c] Concentration(C) with B (Swcnt & Mwcnt)
G=2, M=0.5, K=0.2, Q=0.5, Rd=0.5, Ec=0.1, ϕ=0.05, E1=0.1, δ=0.2, n=1, Sc=0.24, γ=0.5, Q1=0.5, fs=0.1, Pr=0.71

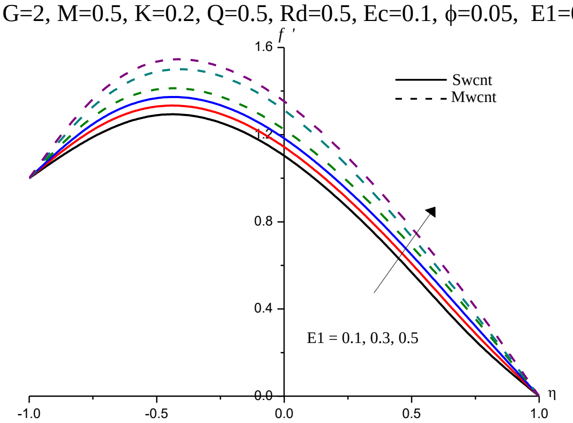

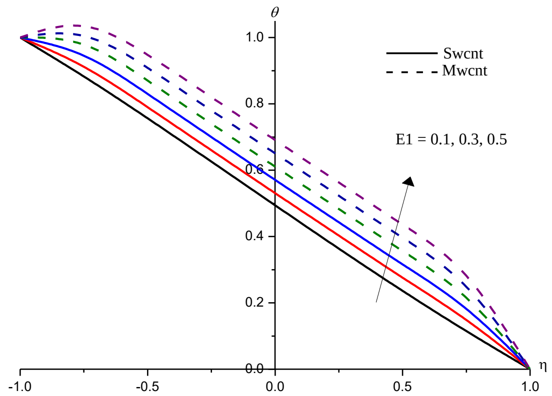

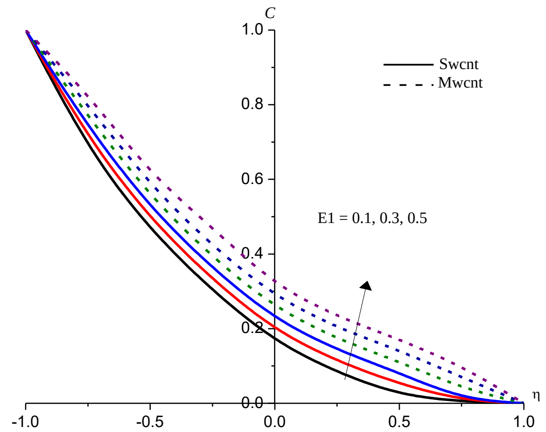

Fig.10 : Variation of [a] Velocity(f'), [b] Temperature(θ), [c] Concentration(C) with E1 (Swcnt & Mwcnt)
G=2, M=0.5, K=0.2, Q=0.5, Rd=0.5, Ec=0.1, ϕ=0.05, B=0.5, δ=0.2, *n*=1, Sc=0.24, γ=0.5, Q1=0.5, fs=0.1, Pr=0.71

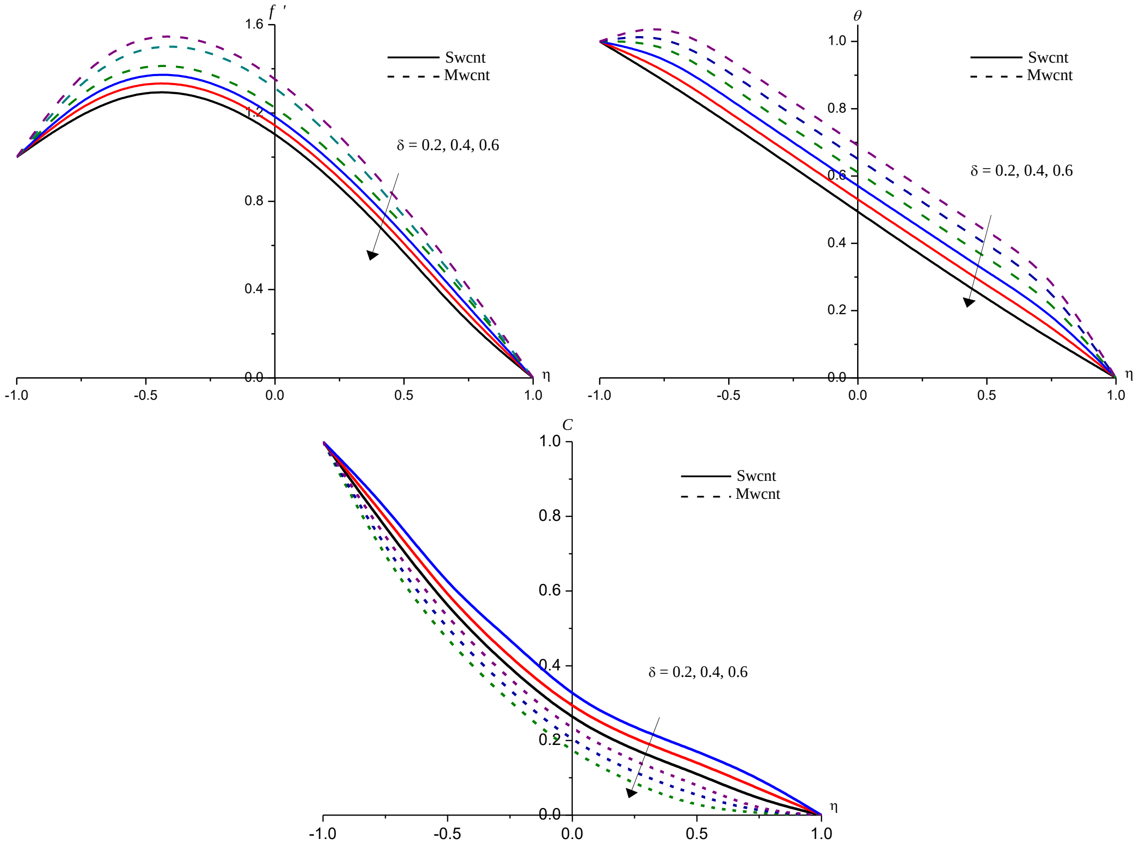

Fig.11 : Variation of [a] Velocity(f'), [b] Temperature(θ), [c] Concentration(C) with δ (Swcnt & Mwcnt)
G=2, M=0.5, K=0.2, Q=0.5, Rd=0.5, Ec=0.1, ϕ=0.05, B=0.5, E1=0.1, *n*=1, Sc=0.24, γ=0.5, Q1=0.5, fs=0.1, Pr=0.71

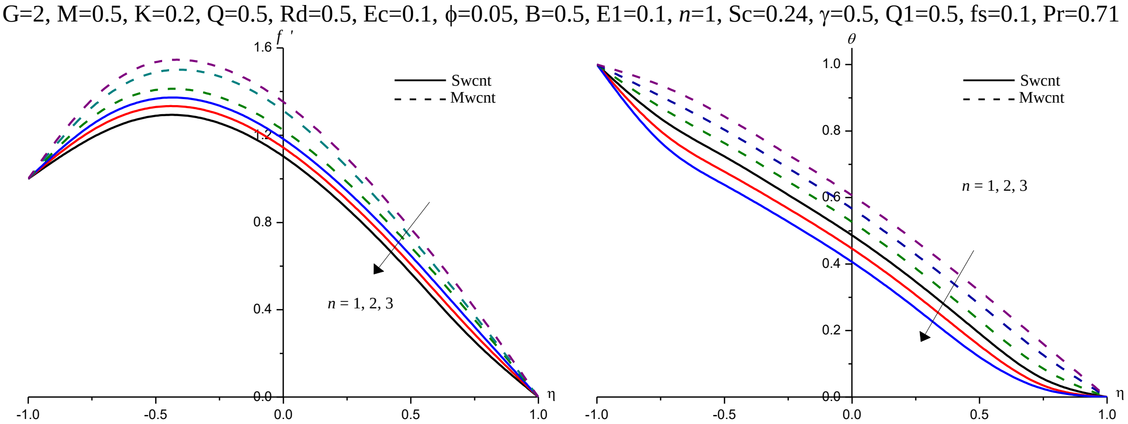

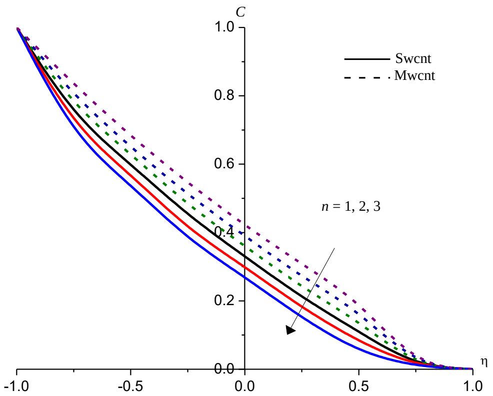

Fig. 12 : Variation of [a] Velocity(f'), [b] Temperature(θ), [c] Concentration(C) with n (Swcnt & Mwcnt)
G=2, M=0.5, K=0.2, Q=0.5, Rd=0.5, Ec=0.1, ϕ=0.05, B=0.5, E1=0.1, δ=0.2, Sc=0.24, γ=0.5, Q1=0.5, fs=0.1, Pr=0.71

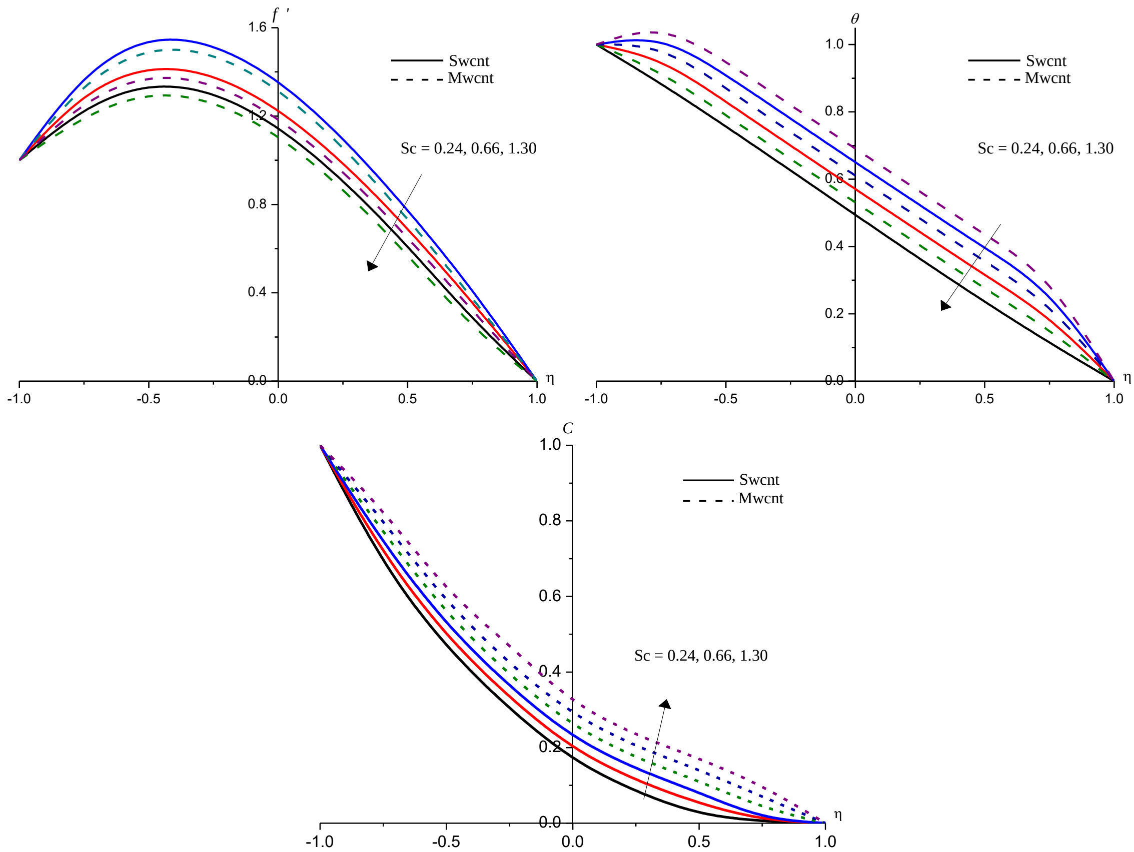

Fig.13 : Variation of [a] Velocity(f'), [b] Temperature(θ), [c] Concentration(C) with Sc (Swcnt & Mwcnt)
G=2, M=0.5, K=0.2, Q=0.5, Rd=0.5, Ec=0.1, ϕ=0.05, B=0.5, E1=0.1, δ=0.2, n=1, γ=0.5, Q1=0.5, fs=0.1, Pr=0.71

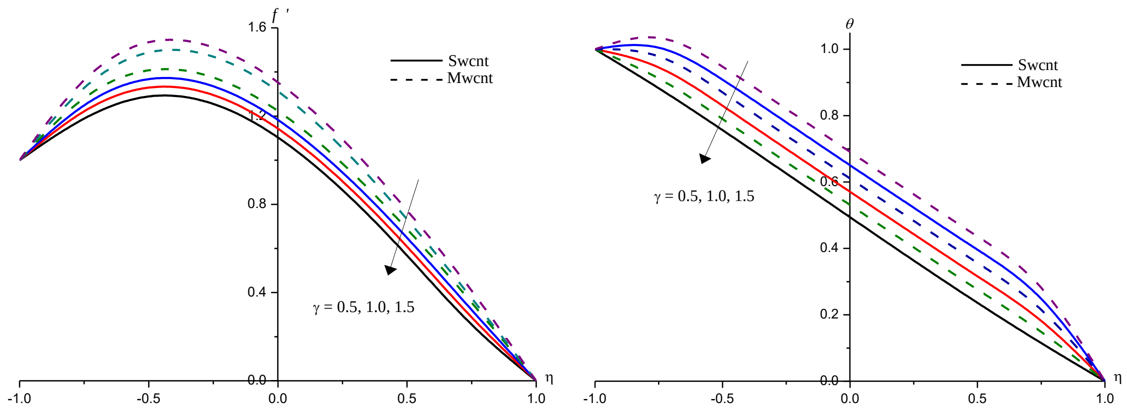

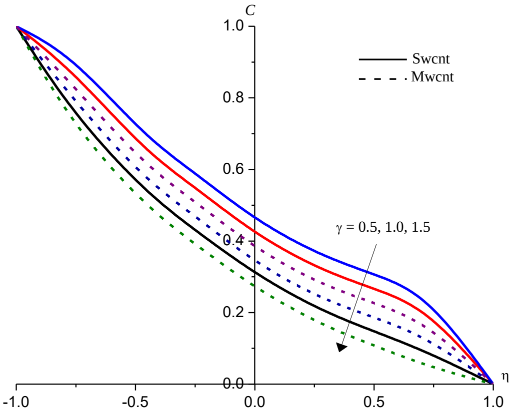

Fig.14 : Variation of [a] Velocity(f'), [b] Temperature(θ), [c] Concentration(C) with γ (Swcnt & Mwcnt)
G=2, M=0.5, K=0.2, Q=0.5, Rd=0.5, Ec=0.1, ϕ=0.05, B=0.5, E1=0.1, δ=0.2, *n*=1, Sc=0.24, Q1=0.5, fs=0.1, Pr=0.71

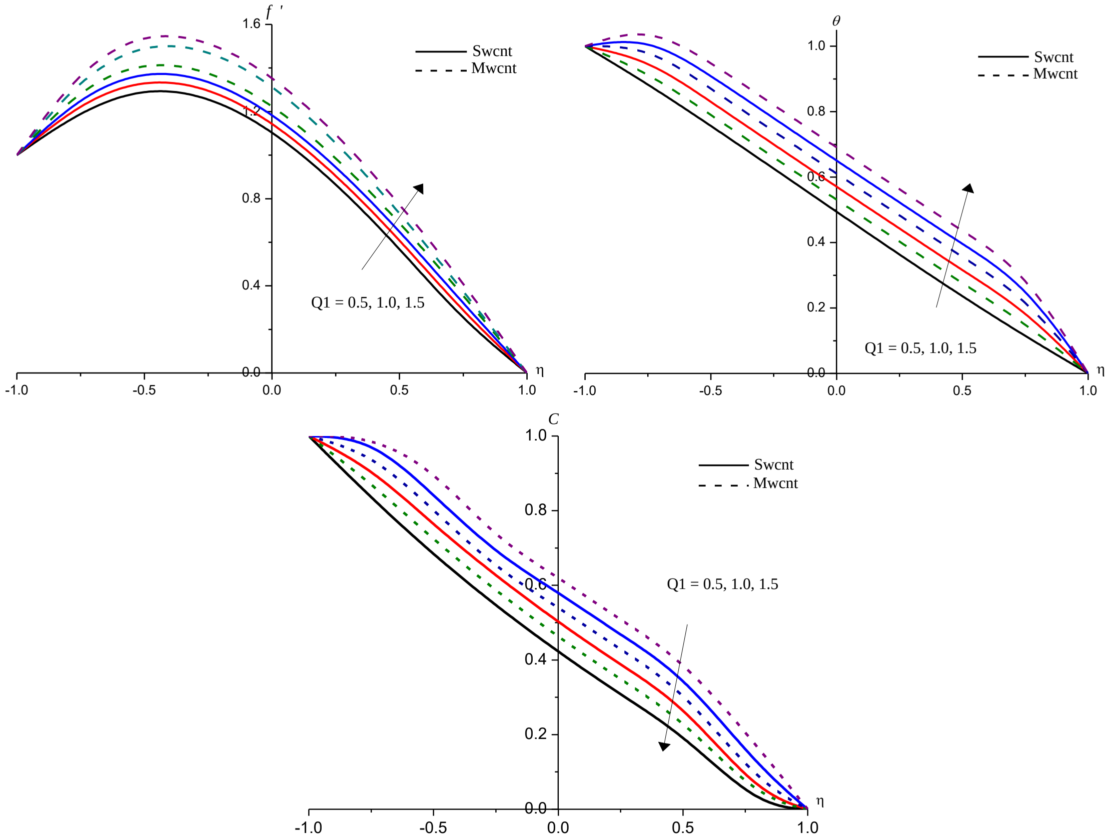

Fig.15 : Variation of [a] Velocity(f'), [b] Temperature(θ), [c] Concentration(C) with Q1 (Swcnt & Mwcnt)
G=2, M=0.5, K=0.2, Q=0.5, Rd=0.5, Ec=0.1, ϕ=0.05,B=0.5, E1=0.1, δ=0.2, *n*=1, Sc=0.24, γ=0.5, fs=0.1, Pr=0.71

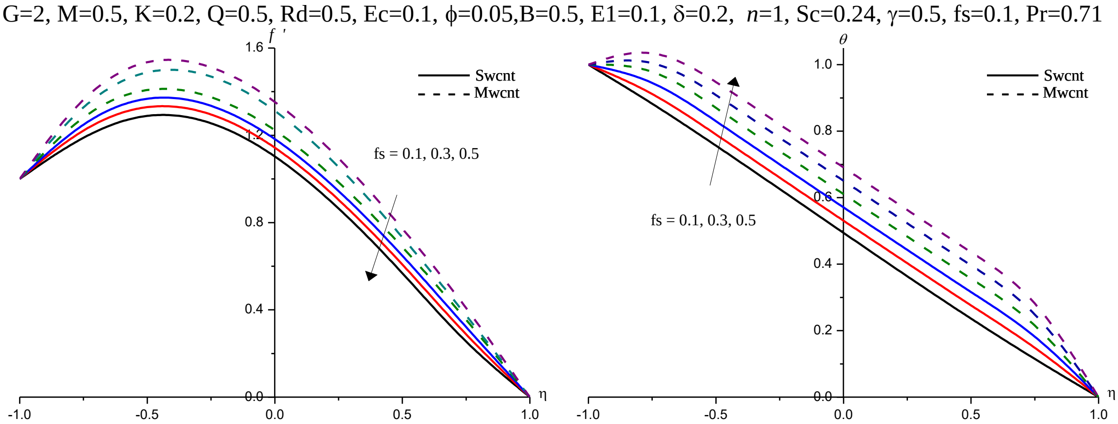

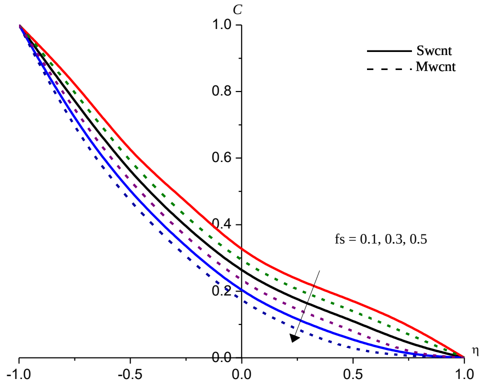

Fig.16 : Variation of [a] Velocity(f'), [b] Temperature(θ), [c] Concentration(C) with fs (Swcnt & Mwcnt)
G=2, M=0.5, K=0.2, Q=0.5, Rd=0.5, Ec=0.1, ϕ=0.05,B=0.5, E1=0.1, δ=0.2, *n*=1, Sc=0.24, γ=0.5, Q1=0.5, Pr=0.71

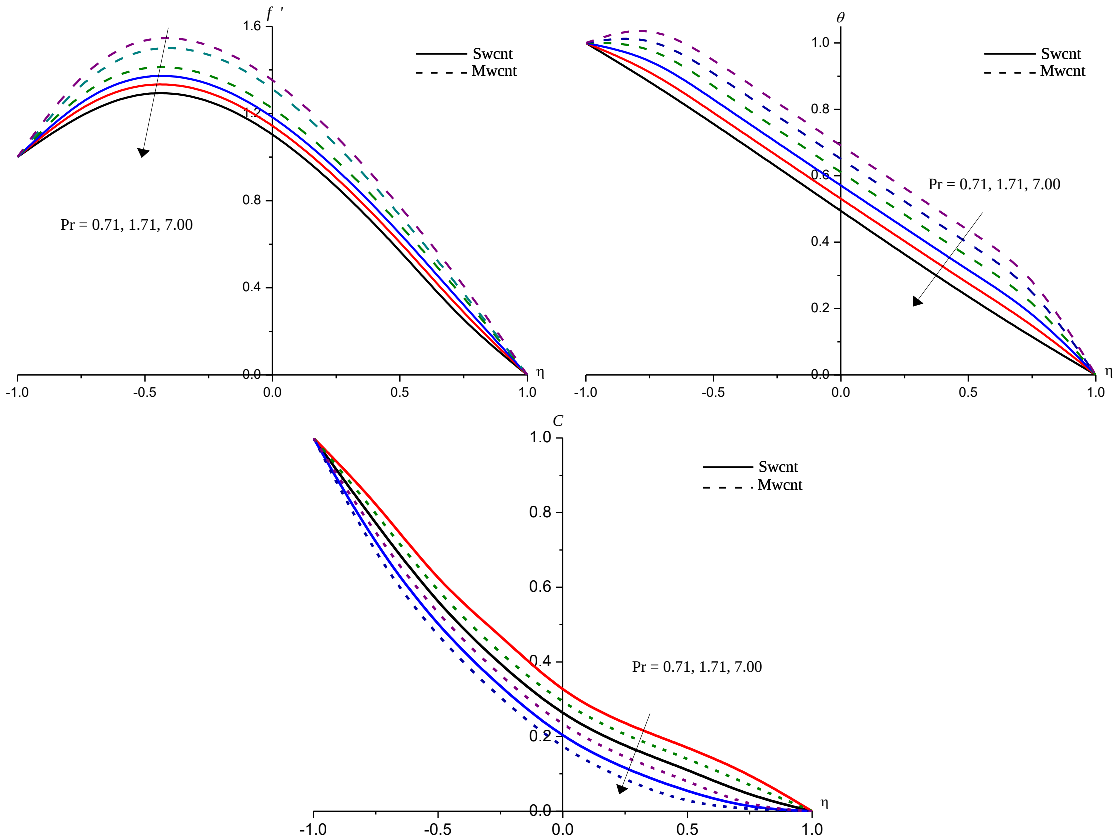

Fig.17 : Variation of [a] Velocity(f'), [b] Temperature(θ), [c] Concentration(C) with Pr (Swcnt & Mwcnt)
G=2, M=0.5, K=0.2, Q=0.5, Rd=0.5, Ec=0.1, ϕ=0.05, B=0.5, E1=0.1, δ=0.2, *n*=1, Sc=0.24, γ=0.5, Q1=0.5, fs=0.1

Table : 1
Skin friction (Cf), Nusselt(Nu) and Sherwood(Sh) Numbers with SWCNT, MWCNT at η = – 1

Parameter		Swcnt-Nanofluid			Mwcnt Nanofluid		
		Cf (-1)	Nu(-1)	Sh(-1)	Cf (-1)	Nu(-1)	Sh(-1)
G	2	1.69773	0.431383	0.691594	1.98253	0.404473	0.702157
	4	2.97928	0.356257	0.740382	4.38631	0.153363	0.811208
	6	4.54742	0.204517	0.806779	6.27749	0.083748	0.892594
M	0.5	1.69773	0.431383	0.691594	1.98253	0.404473	0.702157
	1.0	1.07474	0.448814	0.666506	1.49469	0.410375	0.734564
	1.5	0.62049	0.448853	0.649635	0.83157	0.428993	0.778965
K	0.2	1.69773	0.431383	0.691594	1.98253	0.404457	0.702155
	0.4	1.11518	0.455322	0.666962	1.56181	0.428012	0.685855
	0.6	0.68984	0.466932	0.650291	0.90305	0.448685	0.657126
Rd	1.5	1.69773	0.431383	0.691594	1.98253	0.404473	0.702157

	3.5	1.71432	0.450043	0.692588	2.09847	0.422304	0.708652
	5.0	1.71868	0.457651	0.692858	2.19307	0.450040	0.802879
Ec	0.1	1.69773	0.431383	0.691594	1.98253	0.404473	0.702157
	0.2	1.84167	0.218395	0.699777	2.73462	0.543586	0.746775
	0.3	2.08308	0.146500	0.714044	2.83182	0.780605	0.754048
Q	0.5	1.69773	0.431383	0.691594	1.98253	0.404473	0.702157
	1.0	1.88357	0.115931	0.701823	2.10636	0.234751	0.708957
	1.5	1.89344	0.111086	0.702391	2.23004	0.075444	0.715938
B	0.5	1.69773	0.431383	0.691594	1.98253	0.404473	0.702157
	1.0	2.33277	0.391943	0.708343	3.17737	0.273825	0.747297
	1.5	3.49309	0.268935	0.740503	4.22037	0.153857	0.768108
E1	0.1	1.69773	0.431327	0.691594	1.98253	0.404473	0.702159
	0.3	1.69786	0.431379	0.688713	2.23023	0.404202	0.713074
	0.5	1.69829	0.431704	0.686521	2.98286	0.404192	0.757106
ϕ	0.05	1.69773	0.431385	0.691554	1.98253	0.404455	0.702157
	0.10	1.69763	0.431534	0.694364	2.22987	0.403417	0.719021
	0.15	1.69725	0.431643	0.696932	2.98234	0.402742	0.727523
δ	0.2	1.69773	0.431382	0.691535	1.98253	0.404473	0.702157
	0.4	1.11406	0.531291	0.668445	1.72126	0.461013	0.694244
	0.6	0.64024	0.622932	0.650123	1.03135	0.559263	0.663916
n	0.25	1.69773	0.431383	0.691594	1.98253	0.404475	0.702157
	0.50	1.69766	0.431481	0.693759	2.22991	0.404237	0.718328
	0.75	1.69758	0.431579	0.695921	2.98235	0.404072	0.726505
γ	0.5	1.69773	0.431383	0.691594	1.98253	0.404473	0.702157
	1.0	1.69496	0.434913	0.757748	2.22578	0.409931	0.782450
	1.5	1.69134	0.439556	1.847295	2.47475	0.412693	0.857418
Q1	0.5	1.69773	0.431383	0.691594	1.98717	0.404473	0.702157
	1.0	1.84142	0.176151	0.699455	1.98253	0.218032	0.728737
	1.5	2.33816	0.078496	0.707722	2.44949	0.108156	0.732134
fs	0.2	1.48271	0.4412152	0.682873	1.73826	0.417295	0.691995
	0.4	1.69773	0.4313835	0.691594	2.23004	0.407556	0.715938
	0.6	2.14403	0.4062616	0.710715	2.51564	0.369598	0.725688
Pr	0.71	1.91833	0.1944158	0.704048	2.23342	0.189853	0.7164014
	3.71	1.87918	0.2291865	0.701778	2.49001	0.100698	0.7314498
	7.00	1.69773	0.4313834	0.691594	2.68253	0.094735	0.7521576
Sc	0.24	1.91833	0.1944158	0.7040485	2.23342	0.189853	0.7164014
	0.66	1.77654	0.1675439	0.6543420	2.20678	0.198776	0.6654389
	1.30	1.56478	0.1546777	0.5543222	1.89765	0.205678	0.5748999

Table : 2

Skin friction (Cf), Nusselt(Nu) and Sherwood(Sh) Numbers with SWCNT, MWCNT at η = + 1

Parameter		Swcnt-Nanofluid			Mwcnt Nanofluid		
		Cf (+1)	Nu(+1)	Sh(+1)	Cf (+1)	Nu(+1)	Sh(+1)
G	2	-1.46579	0.434498	0.3949706	-1.55436	0.452229	0.388748
	4	-1.88919	0.473246	0.3667581	-2.43968	0.705134	0.328075
	6	-2.44821	0.542894	0.3309135	-2.74956	0.876886	0.288494
M	0.5	-1.46579	0.434494	0.3949706	-1.55436	0.452229	0.388748
	1	-1.21899	0.420588	0.4108631	-1.35555	0.565988	0.400787
	1.5	-1.05371	0.415078	0.4217258	-0.27514	0.629388	0.417571
K	0.2	-1.46579	0.434455	0.3949706	-1.34935	0.452229	0.388974
	0.4	-1.20958	0.417866	0.4109244	-0.69778	0.562549	0.399449
	0.6	-1.03755	0.408455	0.4218971	-0.59748	0.621789	0.417976
Rd	1.5	-1.46579	0.434498	0.3949706	-1.55436	0.452229	0.388748
	3.5	-1.47322	0.481028	0.3942675	-1.40024	0.486733	0.384738
	5.0	-1.47534	0.496813	0.3940694	-0.87586	0.503205	0.382166
Ec	0.1	-1.46579	0.434498	0.3949706	-1.55436	0.452229	0.388748
	0.2	-1.52077	0.634333	0.3897778	-1.84898	1.040797	0.362158
	0.3	-1.61206	0.938304	0.3809034	-2.09602	1.321522	0.357782
Q	0.5	-1.46579	0.434493	0.3949447	-1.55436	0.452229	0.388789

	1.0	-1.53112	0.555397	0.3888657	-1.36006	0.520747	0.384706
	1.5	-1.53481	0.563892	0.3885156	-0.95562	0.589722	0.380575
B	0.5	-1.46579	0.434498	0.3949706	-1.55436	0.452229	0.388874
	1.0	-1.49596	0.446451	0.3873763	-1.72509	0.625945	0.366009
	1.5	-1.56996	0.476495	0.3731194	-1.85819	0.716478	0.359193
E1	0.1	-1.46579	0.434449	0.3949444	-1.55436	0.452229	0.388794
	0.3	-1.46584	0.434585	0.3961156	-1.64735	0.589839	0.381688
	0.5	-1.46587	0.434651	0.3969843	-1.87832	0.652391	0.360773
ϕ	0.05	-1.46579	0.434498	0.3949706	-1.55436	0.452229	0.388748
	0.10	-1.20902	0.371872	0.4097697	-1.41674	0.442261	0.394025
	0.15	-0.993373	0.322509	0.4220254	-1.33259	0.359733	0.413356
δ	0.2	-1.46579	0.431383	0.6915355	-1.55436	0.404473	0.702155
	0.4	-1.46576	0.431531	0.6943967	-1.34721	0.404517	0.719025
	0.6	-1.46553	0.431822	0.6969367	-0.87818	0.404772	0.727526
n	1	-1.46579	0.434459	0.3949723	1.55436	0.452229	0.388747
	2	-1.46577	0.434463	0.3944012	-1.64723	0.589642	0.379912
	3	-1.46564	0.434384	0.3938334	-2.87819	0.602118	0.367612
Sc	0.24	-1.46579	0.434498	0.3949706	-1.55436	0.452229	0.388764
	0.66	-1.46075	0.423923	0.2707555	-1.63787	0.574795	0.244446
	1.30	-1.45707	0.416435	0.1911752	-1.86918	0.632806	0.178169
γ	0.5	-1.46579	0.434490	0.3949766	-1.55436	0.452229	0.388764
	1.0	-1.46483	0.432415	0.3702162	-1.64564	0.450871	0.356275
	1.5	-1.46351	0.429697	0.3382463	-1.87602	0.447341	0.332865
Q1	0.5	-1.46579	0.434494	0.3949706	-1.55436	0.452226	0.388743
	1.0	-1.51605	0.526324	0.3902891	-1.73024	0.505812	0.37313
	1.5	-1.56765	0.617733	0.3854144	-1.99352	0.639918	0.370013
fs	0.2	-1.39119	0.42857558	0.4002427	-1.46792	0.444813	0.394827
	0.4	-1.46579	0.4344908	0.3949752	-1.64728	0.459722	0.380574
	0.6	-1.62994	0.4488046	0.3835271	-1.99945	0.471416	0.37687
Pr	0.71	-1.54767	0.677067	0.3872356	-1.65388	0.681348	0.3799827
	3.71	-1.53288	0.628181	0.3886534	-1.75183	0.830985	0.3801141
	7.00	-1.46579	0.4344907	0.4497065	-1.87825	0.952229	0.3887489

References

[1]. Agarwal. S. Bhadauri, B.S. Siddheshwar, P.G (2011): Thermal instability of a nanofluid saturating a rotating anisotropic porous medium, STRPM, vol.2, pp:53–64

[2]. Ahmed N., Mohyud-Din S. T., and Hassan S. M., "Flow and heat transfer of nanofluid in an asymmetric channel with expanding and contracting walls suspended by carbon nanotubes: A numerical investigation," Aerosp. Sci. Technol., vol. 48, pp. 53–60, 2016. DOI: 10.1016/j.ast.2015.10.022.

[3]. Buongiorno. J (2006): Convective transport in nanofluids," ASME J Heat Tran vol.128, pp:240–250

[4]. Das UN, Deka R. Soundalgekar VM. Effect of mass transfer on flow past an impulsively started infinite vertical plate with constant heat flux and chemical reaction. Forsch ingenieurwes 1994;60:284-7.

[5]. Ding Y, Alias H, Wen D, Williams RA. Heat transfer of aqueous suspensions of carbon nanotubes (CNT nanofluids). International Journal of Heat and Mass Transfer. 2006;49(1):240-250

[6]. Gayathri, P : Impact of Variable Viscosity, Activation Energy on MHD Mixed Convective Heat and Mass Transfer Flow of a Nanofluid in a Cylindrical Annulus, *YMER :* Vol.21. Issue:4, PP:211-223, April-2022, ISSN : 0044-0477, www.ymerdigital.com

[7]. Ghadimi. A, Saidur. R, Metselaar. H. S. C (2011): A review of nanofluid stability properties and charac terization in stationary conditions, Int. J Heat Mass Tran. vol.54(17-18), pp:4051–4068.

[8]. Gireesha B.J., M. Archana, B. Mahanthesh, Prasannakumara B.C., "Exploration of activationenergy and binary chemical reaction effects on nano Casson fluid flow with

thermal and exponentialspace-based heat source", Multidiscipline Modeling in Materials and Structures, V.15 : 1, pp.227-245, (2019)

[9]. Hazarika S., Ahmed S.: Study of Carbon Nanotubes with a Casson Fluid in a Vertical Channel of Porous Media under MHD and Dufour Effect, Journal of Scientific Research, 13 (1), 31-45 (2021), web: www.banglajol.info/index.php/JSR

[10]. Ibrahim M., and Khan M. I., “Mathematical modeling and analysis of SWCNT-Water and MWCNT-Water flow over a stretchable sheet,” Comput. Meth. Prog. Biomed., vol. 187, pp. 105222, 2020. DOI: 10.1016/j.cmpb.2019.105222.

[11]. Ijaj Khan M, Sohail A, Khan, Hayat T, Imran Khan M and Alsaedi A : Arrchenius activation energy impact in binary chemically reactive flow of TiO_2-Cu-H2O hybird nanomaterial, International Journal of Chemical Reactor Engineering, (2018), DOI:10.1515/ijcre-2018-0183

[12]. Jingqi Li, Chao Zhao, Qingxiao Wang, Qiang Zhang, Zhihong Wang, X.X. Zhang, A.I. Abutaha, H.N. Alshareef : Vertically aligned carbon nanotube field-effect transistors, Sci.Verse Science Direct, 50, (2012), pp.4628-4632, Elsevier www.elsevier.com/locate/carbon,http://dx.doi.org/10.1016/j.carbon. 2012.05.049

[13]. Kafoussias NG. Williams EW. Effects of temperature-dependent viscosity on free-forced convective laminar boundary layer flow past a vertical isothermal flat plate. Acta Mech 1995;110:123-137.

[14]. Khan M.I.T, Hayat M, Khan I, and Alsaedi A: Activatio Energy impact in Nonlinear Radiative Stagnation Point Flow of Cross Nanofluid, Int.Communiations Heat Massachusetts Transfer, V.91, pp.216-224, (2018)

[15]. Kiblinski. P, Phillpot. S. R and Choi. S. U. S (2002): J.A.Eastman,”Mechanism of heat flow is suspensions of nanosized particles (nanofluids), Int. J Heat Mass Tran, vol.42, pp:855–863.

[16]. Ko GH, Heo K, Lee K, Kim DS, Kim C, Sohn Y, Choi M. An experimental study on the pressure drop of nanofluids containing carbon nanotubes in a horizontal tube. International Journal of Heat and Mass Transfer. 2007;50(23):4749-4753

[17]. Nguyen. C. T, Roy. G, Gauthier. C and Galanis. N (2007) Heat transfer enhancement using Al_2O_3–water nanofluid for an electronic liquid cooling system, Appl. Thermo Eng, vol.27, pp:1501–1506.

[18]. Oztop. H. F and Abu-Nada. E (2008): Numerical study of natural convection in partially heated rectangular enclosures filled with nanofluids.,Int.J.Heat and Fluid Flow., V.29,pp.1326-1336.

[19]. Pantokratoras A. Further results on the variable viscosity on flow and heat transfer to a continuous moving flat plate. Int. J. Eng. Sci. 2004;42:1891-1896.

[20]. Pantokratoras A. Laminar free-convection over a vertical isothermal plate with uniform blowing or suction in water with variable physical properties. Int.J.Heat Mass. Transfer 2002;45:963-977.

[21]. Pantokratoras A. The Falkner-Skan with constant wall temperature and variable viscosity. Int. J. Thermal Sciences 2006;45:378-89.

[22]. Saida Rashid, Tasawar Hayat, Sumaira Qayyum, Muhammad Ayub, Ahmed Alsaedi, "Threedimensionalrotating Darcy–Forchheimer flow with activation energy", Int. Journal of Numerical Methods for Heat & Fluid Flow, 29 : 3, pp.935-948, (2019)

[23]. Sandhya G, Sreelakshmi K, Sarojamma G, : Effect of Arrhenius activation energy and dual stratifications on the MHD flow of a Maxwell nanofluid with viscous heating, The International Journal of Engineering and Science (IJES), ISSN (e): 2319 – 1813 ISSN (p): 23-19 – 1805, pp.55-60, (2020)

[24]. Shamshuddin M. D., Isaac Lare Animasaun, Sulyman Olakunle Salawu and Pudi Srinivasa Rao: Dynamics of ethylene glycol conveying MWCNTs and ethylene glycol conveying SWCNTs: Significant joule heating and thermal radiation, Numerical Heat

Transfer, Part A: Applications (2023), https://doi.org/10.1080/10407782.2023.2195130

[25]. Sheikholeslami M., “Numerical investigation of solar system equipped with innovative turbulator and hybrid nanofluid,” Sol. Energy Mater. Sol. Cells, vol. 243, pp. 111786, 2022. DOI: 10.1016/j.solmat.2022.111786.

[26]. Youngki Yoon, James Fodor, and Jing Guo : A Computational Study of Vertical Partial Gate Carbon Nanotube FETs, IEEE Transactions on Electron Devices , Volume: 55, Issue: 1, January 2008, Pp. 283 – 288, https://doi.org/10.1109/TED.2007.910561

[27]. Zeeshan A., Shehzad N., Ellahi R., “Analysis of activation energy in Couette-Poiseuille flow of nanofluid in the presence of chemical reaction and convective boundary conditions”, Results in Physics,V.8 ,pp. 502–512(2018).